Research Article | Vol. 7, No. 11 | 1 Nov 2017 | OPTICAL MATERIALS EXPRESS 4192
Optical Materials EXPRESS

Synthesis, spectroscopy, and efficient laser operation of "mixed" sesquioxide Tm:$(Lu,Sc)_2O_3$ transparent ceramics

Wei Jing,[1] Pavel Loiko,[2] Josep Maria Serres,[3] Yicheng Wang,[4] Elena Vilejshikova,[5] Magdalena Aguiló,[3] Francesc Díaz,[3] Uwe Griebner,[4] Hui Huang,[1,6] Valentin Petrov,[4] and Xavier Mateos[3,*]

[1]*Institute of Chemical Materials, China Academy of Engineering Physics, 64 Mianshan Road, 621900 Mianyang, China*
[2]*ITMO University, 49 Kronverkskiy Pr., 197101 St. Petersburg, Russia*
[3]*Física i Cristal·lografia de Materials i Nanomaterials (FiCMA-FiCNA)-EMaS, Departamento Química Física i Inòrganica, Universitat Rovira i Virgili (URV), Campus Sescelades, E-43007 Tarragona, Spain*
[4]*Max Born Institute for Nonlinear Optics and Short Pulse Spectroscopy, Max-Born-Str. 2a, D-12489 Berlin, Germany*
[5]*Center for Optical Materials and Technologies (COMT), Belarusian National Technical University, 65/17 Nezavisimosti Ave., 220013 Minsk, Belarus*
[6]*huanghui@caep.cn*
[*]*xavier.mateos@urv.cat*

Abstract: A novel transparent 4.76 at.% Tm:$(Lu_{2/3}Sc_{1/3})_2O_3$ "mixed" sequioxide ceramic is synthesized by hot isostatic pressing (HIP) at 1800 °C / 195 MPa in an Ar atmosphere. Its structure is studied by scanning electron microscopy, X-ray diffraction, and Raman spectroscopy. The spectroscopic properties of the Tm^{3+} ion are described within the Judd-Ofelt theory, which resulted in intensity parameters of $\Omega_2 = 2.429$, $\Omega_4 = 1.078$ and $\Omega_6 = 0.653$ [10^{-20} cm^2]. For the $^3F_4 \rightarrow {}^3H_6$ transition, the maximum stimulated-emission cross-section σ_{SE} is 7.15×10^{-21} cm^2 at 1951 nm. The radiative lifetime of the $^3F_4$ state is 4.01 ms. Under diode-pumping at 802 nm, a microchip Tm:$(Lu,Sc)_2O_3$ ceramic laser generated ~1 W at 2100 nm with a slope efficiency of 24%. The spectroscopic and laser properties of the Tm:$(Lu,Sc)_2O_3$ ceramic are compared with those of a Tm:$LuScO_3$ single crystal. The ceramic exhibits very broad and flat gain cross sections, which is promising for ultrashort pulse generation.

OCIS codes: (140.3380) Laser materials; (300.0300) Spectroscopy; (140.3480) Lasers, diode-pumped.

References and links

1. C. Kränkel, "Rare-earth-doped sesquioxides for diode-pumped high-power lasers in the 1-, 2-, and 3-μm spectral range," IEEE J. Sel. Top. Quantum Electron. **21**(1), 1602013 (2015).
2. R. Peters, C. Kränkel, S. T. Fredrich-Thornton, K. Beil, K. Petermann, G. Huber, O. H. Heckl, C. R. E. Baer, C. J. Saraceno, T. Südmeyer, and U. Keller, "Thermal analysis and efficient high power continuous-wave and mode-locked thin disk laser operation of Yb-doped sesquioxides," Appl. Phys. B **102**(3), 509–514 (2011).
3. P. A. Loiko, K. V. Yumashev, R. Schödel, M. Peltz, C. Liebald, X. Mateos, B. Deppe, and C. Kränkel, "Thermo-optic properties of Yb:Lu_2O_3 single crystals," Appl. Phys. B **120**(4), 601–607 (2015).
4. K. Petermann, G. Huber, L. Fornasiero, S. Kuch, E. Mix, V. Peters, and S. A. Basun, "Rare-earth-doped sesquioxides," J. Lumin. **87–89**, 973–975 (2000).
5. P. Koopmann, R. Peters, K. Petermann, and G. Huber, "Crystal growth, spectroscopy and highly efficient laser operation of thulium-doped Lu_2O_3 around 2 μm," Appl. Phys. B **102**(1), 19–24 (2011).
6. P. Koopmann, S. Lamrini, K. Scholle, P. Fuhrberg, K. Petermann, and G. Huber, "Efficient diode-pumped laser operation of Tm:Lu_2O_3 around 2 μm," Opt. Lett. **36**(6), 948–950 (2011).
7. P. Koopmann, S. Lamrini, K. Scholle, M. Schäfer, P. Fuhrberg, and G. Huber, "Holmium-doped Lu_2O_3, Y_2O_3, and Sc_2O_3 for lasers above 2.1 μm," Opt. Express **21**(3), 3926–3931 (2013).
8. A. Schmidt, P. Koopmann, G. Huber, P. Fuhrberg, S. Y. Choi, D.-I. Yeom, F. Rotermund, V. Petrov, and U. Griebner, "175 fs Tm:Lu_2O_3 laser at 2.07 μm mode-locked using single-walled carbon nanotubes," Opt. Express **20**(5), 5313–5318 (2012).

#307878 https://doi.org/10.1364/OME.7.004192
Journal © 2017 Received 25 Sep 2017; revised 25 Oct 2017; accepted 26 Oct 2017; published 31 Oct 2017

Optical Materials EXPRESS

9. M. Tokurakawa, A. Shirakawa, K. Ueda, H. Yagi, M. Noriyuki, T. Yanagitani, and A. A. Kaminskii, "Diode-pumped ultrashort-pulse generation based on Yb^{3+}:Sc_2O_3 and Yb^{3+}:Y_2O_3 ceramic multi-gain-media oscillator," Opt. Express **17**(5), 3353–3361 (2009).
10. A. A. Lagatsky, P. Koopmann, P. Fuhrberg, G. Huber, C. T. A. Brown, and W. Sibbett, "Passively mode locked femtosecond Tm:Sc_2O_3 laser at 2.1 μm," Opt. Lett. **37**(3), 437–439 (2012).
11. R. Peters, C. Kränkel, K. Petermann, and G. Huber, "Broadly tunable high-power Yb:Lu_2O_3 thin disk laser with 80% slope efficiency," Opt. Express **15**(11), 7075–7082 (2007).
12. C. R. E. Baer, C. Kränkel, C. J. Saraceno, O. H. Heckl, M. Golling, R. Peters, K. Petermann, T. Südmeyer, G. Huber, and U. Keller, "Femtosecond thin-disk laser with 141 W of average power," Opt. Lett. **35**(13), 2302–2304 (2010).
13. R. C. Stoneman and L. Esterowitz, "Efficient, broadly tunable, laser-pumped Tm:YAG and Tm:YSGG cw lasers," Opt. Lett. **15**(9), 486–488 (1990).
14. P. Loiko and M. Pollnau, "Stochastic model of energy-transfer processes among rare-earth ions. Example of Al_2O_3:Tm^{3+}," J. Phys. Chem. C **120**(46), 26480–26489 (2016).
15. P. Koopmann, S. Lamrini, K. Scholle, P. Fuhrberg, K. Petermann, and G. Huber, "Laser operation and spectroscopic investigations of Tm:$LuScO_3$," *in CLEO/Europe - EQEC 2011* (Optical Society of America, 2011), P. CA1_4.
16. A. A. Lagatsky, P. Koopmann, O. L. Antipov, C. T. A. Brown, G. Huber, and W. Sibbett, "Femtosecond pulse generation with Tm-doped sesquioxides," *in CLEO/Europe - EQEC 2011* (Optical Society of America, 2013), P. CA_6_3.
17. R. Peters, C. Krankel, K. Petermann, and G. Huber, "Crystal growth by the heat exchanger method, spectroscopic characterization and laser operation of high-purity Yb:Lu_2O_3," J. Cryst. Growth **310**(7–9), 1934–1938 (2008).
18. O. L. Antipov, A. A. Novikov, N. G. Zakharov, and A. P. Zinov'ev, "Optical properties and efficient laser oscillation at 2066 nm of novel Tm:Lu_2O_3 ceramics," Opt. Mater. Express **2**(2), 183–189 (2012).
19. O. L. Antipov, A. A. Novikov, N. G. Zakharov, A. P. Zinoviev, H. Yagi, N. V. Sakharov, M. V. Kruglova, M. O. Marychev, O. N. Gorshkov, and A. A. Lagatskii, "Efficient 2.1-μm lasers based on Tm^{3+}:Lu_2O_3 ceramics pumped by 800-nm laser diodes," Phys. Status Solidi **10**(6), 969–973 (2013).
20. A. A. Lagatsky, O. L. Antipov, and W. Sibbett, "Broadly tunable femtosecond Tm:Lu_2O_3 ceramic laser operating around 2070 nm," Opt. Express **20**(17), 19349–19354 (2012).
21. E. J. Saarinen, E. Vasileva, O. Antipov, J.-P. Penttinen, M. Tavast, T. Leinonen, and O. G. Okhotnikov, "2-μm Tm:Lu_2O_3 ceramic disk laser intracavity-pumped by a semiconductor disk laser," Opt. Express **21**(20), 23844–23850 (2013).
22. X. Xu, Z. Hu, D. Li, P. Liu, J. Zhang, B. Xu, and J. Xu, "First laser oscillation of diode-pumped Tm^{3+}-doped $LuScO_3$ mixed sesquioxide ceramic," Opt. Express **25**(13), 15322–15329 (2017).
23. L. Laversenne, Y. Guyot, C. Goutaudier, M. T. Cohen-Adad, and G. Boulon, "Optimization of spectroscopic properties of Yb^{3+}-doped refractory sesquioxides: cubic Y_2O_3, Lu_2O_3 and monoclinic Gd_2O_3," Opt. Mater. **16**(4), 475–483 (2001).
24. N. D. Todorov, M. V. Abrashev, V. Marinova, M. Kadiyski, L. Dimowa, and E. Faulques, "Raman spectroscopy and lattice dynamical calculations of Sc_2O_3 single crystals," Phys. Rev. B **87**(10), 104301 (2013).
25. O. Antipov, A. Novikov, S. Larin, and I. Obronov, "Highly efficient 2 μm CW and Q-switched Tm^{3+}:Lu_2O_3 ceramics lasers in-band pumped by a Raman-shifted erbium fiber laser at 1670 nm," Opt. Lett. **41**(10), 2298–2301 (2016).
26. B. R. Judd, "Optical absorption intensities of rare-earth ions," Phys. Rev. **127**(3), 750–761 (1962).
27. G. S. Ofelt, "Intensities of crystal spectra of rare-earth ions," J. Chem. Phys. **37**(3), 511–520 (1962).
28. L. Zhang, H. Lin, G. Zhang, X. Mateos, J. M. Serres, M. Aguiló, F. Díaz, U. Griebner, V. Petrov, Y. Wang, P. Loiko, E. Vilejshikova, K. Yumashev, Z. Lin, and W. Chen, "Crystal growth, optical spectroscopy and laser action of Tm^{3+}-doped monoclinic magnesium tungstate," Opt. Express **25**(4), 3682–3693 (2017).
29. C. M. Dodson and R. Zia, "Magnetic dipole and electric quadrupole transitions in the trivalent lanthanide series: Calculated emission rates and oscillator strengths," Phys. Rev. B **86**(12), 125102 (2012).
30. P. Koopmann, "Thulium- and holmium-doped sesquioxides for 2 μm lasers," Ph.D. dissertation, Dept. of Physics, University of Hamburg, Hamburg, Germany, 2012.
31. A. S. Yasyukevich, V. G. Shcherbitskii, V. E. Kisel', A. V. Mandrik, and N. V. Kuleshov, "Integral method of reciprocity in the spectroscopy of laser crystals with impurity centers," J. Appl. Spectrosc. **71**(2), 202–208 (2004).
32. B. F. Aull and H. P. Jenssen, "Vibronic interactions in Nd:YAG resulting in nonreciprocity of absorption and stimulated emission cross sections," IEEE J. Quantum Electron. **18**(5), 925–930 (1982).

1. Introduction

Cubic (C-type, bixbyite structure) rare-earth sesquioxides A_2O_3 (where A = Lu, Y, Sc, etc.) are well known host crystals for trivalent laser-active lanthanide ions (Ln^{3+}) such as Yb^{3+}, Tm^{3+} or Ho^{3+} [1]. They feature good thermal and thermo-optical properties (high thermal conductivity, κ = 12.8 W/mK for Lu_2O_3 which is weakly dependent on the Ln^{3+} concentration

Optical Materials EXPRESS

[2], and positive dn/dT coefficients [3]), broad transparency range (0.22-8 μm) and high refractive index (~1.91 for Lu_2O_3 at ~1 μm) [1], one of the lowest maximum phonon frequencies among the oxide matrices [1], as well as broad spectral bands for the Ln^{3+} dopant ions [1,4,5]. Efficient, wavelength-tunable and power-scalable near-IR Ln-doped sesquoxide lasers operating in the continuous-wave (CW) [1,6,7] and mode-locked (ML) regimes (at ~1 and ~2 μm) [8–10] have already been reported. These crystals have also been recognized to be very suitable for thin-disk oscillators [11,12].

Cubic A_2O_3 crystals are in particular attractive for thulium lasers. The Tm^{3+} ion (electronic configuration: $[Xe]4f^{12}$) is known for its emission around 2 μm due to the $^3F_4 \rightarrow {}^3H_6$ 4f-4f electronic transition [13]. This eye-safe emission is used in range-finding, environmental sensing (LIDAR) and medicine. The Tm^{3+} ions can be excited by commercial AlGaAs laser diodes at ~0.8 μm (into the $^3H_4$ state) while the possible cross-relaxation process, $^3H_4 + {}^3H_6 \rightarrow {}^3F_4 + {}^3F_4$, increases the excitation quantum efficiency [14]. In cubic A_2O_3 crystals they feature a strong Stark splitting of the ground state ($^3H_6$), > 800 cm^{-1}, leading to very broad emission and gain spectra extending up to ~2.1 μm [1,5,6] which is much longer than for many other Tm^{3+}-doped oxide crystals. Moreover, this feature can be enhanced in "mixed" Tm:$(Lu_{1-x},Sc_x)_2O_3$ crystals exhibiting a compositional disorder. A 1 at.% Tm:$LuScO_3$ sesquioxide crystal was previously studied in [15] generating a CW output power of 705 mW at ~2.1 μm with a slope efficiency of 55% (under Ti:Sapphire laser pumping). A 155 nm-broad (1960-2115 nm) tuning range of the laser emission was demonstrated [15]. In the ML regime, 105 fs pulses were achieved at 2010 nm using a semiconductor saturable absorber mirror (SESAM) [16]. This corresponded to the shortest pulse duration ever reported for any ML Tm^{3+}:A_2O_3 oscillator, proving the potential of "mixed" crystals for fs ML lasers.

Due to the high melting point of the cubic A_2O_3 crystals (2450 °C for Lu_2O_3), their growth typically requires the use of expensive rhenium (Rh) crucibles [17]. Rh can be the source of crystal coloration. The growth of large-volume highly Tm^{3+}-doped single crystals with high optical quality is complicated. The technology of Tm^{3+}-doped sesquioxide transparent ceramics was proposed as an alternative allowing for an easier and size-scalable production. There are multiple reports on Tm:Lu_2O_3 transparent ceramics [18,19]. In [18], a 2 at.% Tm:Lu_2O_3 ceramic laser generated 26 W at 2066 nm with a slope efficiency of 42%. Bulk fs ML lasers [20] and thin-disk lasers [21] based on Tm:Lu_2O_3 ceramic are also known.

In the present work, we focused on a novel "mixed" Tm:$(Lu_{2/3}Sc_{1/3})_2O_3$ transparent ceramic exhibiting promising potential for ultrafast lasers and amplifiers. We present structural and detailed spectroscopic characterization and compare this ceramic with a Tm:$LuScO_3$ single-crystal. In addition to the ease of fabrication, we demonstrate that this new ceramic material can provide superior laser characteristics in comparison with the previously studied "mixed" Tm:$LuScO_3$ ceramics [22] and single-crystals [15].

2. Fabrication of the Tm:$(Lu,Sc)_2O_3$ ceramics

The Tm:$(Lu,Sc)_2O_3$ ceramics were fabricated by the Hot Isostatic Pressing (HIP) sintering method using powders of Sc_2O_3, Lu_2O_3, and Tm_2O_3 (purity: 99.99%, Alfa Aesar) as raw materials. The raw materials, with a stoichiometric amount of 100 at.% Lu + Sc (taken in a proportion of Lu:Sc = 2:1) and 5 at.% Tm over it, were mixed uniformly by ball milling for 24 h, dried for 6 h at 70 °C, sieved, dry-pressed at 10 MPa, and cold isostactically pressed at 200 MPa. The green bodies of Tm:$(Lu,Sc)_2O_3$ ceramics were firstly pre-sintered at 1750 °C for 10 h under vacuum (pressure, $P < 10^{-3}$ Pa) to densify the preforms. For further densification, the pre-sintered Tm:$(Lu,Sc)_2O_3$ ceramic samples were post-sintered by HIP at 1800 °C for 2 h in an Ar atmosphere (P = 195 MPa) to eliminate the closed pores around the grain boundaries. Finally, the ceramics were annealed at 1500 °C for 10 h in an O_2 atmosphere to eliminate the oxygen vacancies and remove internal stresses. Samples of Tm:$(Lu,Sc)_2O_3$ ceramics with a diameter of 15 mm and a thickness of 5 mm were obtained. Some polished samples are shown in Fig. 1(a). For the spectroscopic experiments, 3 × 3 × 3

Optical Materials EXPRESS

mm^3 cubes were cut from the prepared samples and polished to laser-grade quality. The composition of the ceramics can be represented as 4.76 at.% Tm:$(Lu_{2/3}Sc_{1/3})_2O_3$.

The polycrystalline phase of the samples was analyzed at room-temperature (RT, 293 K) by X-ray diffraction (XRD) (D2 PHASER, Bruker Co. Ltd), using Cu Kα radiation. The experiment was carried out in the 2θ = 10-80° range with a step of 0.02° and a scan speed of 0.1°/min. As shown in Fig. 1(b), the measured diffraction pattern agrees with the JCPDS card No. 04-002-0541 of cubic $LuScO_3$ (C-type structure, sp. gr. $Ia\bar{3}$ - T^7_h, No. 206). Based on the position of the XRD peaks, the lattice constant of the Tm:$(Lu,Sc)_2O_3$ ceramic is a = 10.3683 Å (Z = 16, calculated density, ρ_{calc} = 7.493 g/cm^3), which is larger than that for the standard $LuScO_3$ crystal (a = 10.105 Å). This is attributed to the larger fraction of Lu^{3+} with larger ionic radius (R_{Lu} = 0.861 Å for VI-fold O^{2-} coordination) as compared to Sc^{3+} (R_{Sc} = 0.745 Å), as well as the Tm^{3+} doping (R_{Tm} = 0.88 Å).

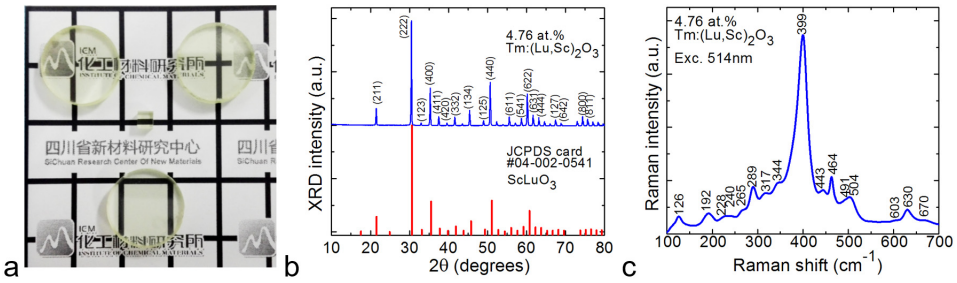

Fig. 1. Some of the fabricated 4.76 at.% Tm:$(Lu,Sc)_2O_3$ ceramics (laser-grade-polished ceramic disks) (a); X-ray diffraction (XRD) pattern (in *blue*) compared to the standard pattern of $ScLuO_3$ (in *red*) (b); Raman spectrum, excitation wavelength: 514 nm (c).

The vibronic properties of the ceramics were studied with Raman spectroscopy, Fig. 1(c). We used a Renishaw inVia confocal Raman microscope with an excitation wavelength λ_{exc} = 514 nm. The Raman spectrum of the Tm:$(Lu,Sc)_2O_3$ ceramic is typical for cubic sesquioxides A_2O_3 [23] while significant broadening of the Raman bands is observed as compared to single crystals. The most intense Raman band is centered at 399 cm^{-1}. It has an asymmetric shape with a full width at half maximum (FWHM) of 32 cm^{-1} and is composed of several poorly resolved components. A factor group analysis predicts the following irreducible representations at the Γ-point: $\Gamma_{total} = 4A_g + 4E_g + 14F_g + 5A_u + 5E_u + 17F_u$ of which 22 modes (A_g, E_g and F_g) are Raman-active, 17 modes (F_u) are IR-active and the rest are silent [24]. We have resolved 16 Raman bands as indicated in Fig. 1(c). While the strongest band is typically ascribed to the $A_g + F_g$ vibrations, the assignment of the modes is complicated [24].

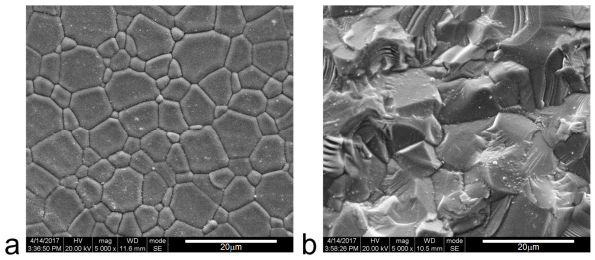

Fig. 2. Field-emission scanning electron microscopy (SEM) images of a polished (a) and a fracture (b) surface of the 4.76 at.% Tm:$(Lu,Sc)_2O_3$ ceramic. The scale bar in (a,b) is 20 μm.

The morphology of a polished surface and a fracture surface was characterized by field-emission scanning electron microscopy (SEM, Inspect F, FEI). The Tm:$(Lu,Sc)_2O_3$ sample is almost pore-free, see Fig. 2. The grain boundaries are clean and there is almost no secondary phase at the grain boundaries or inner grains. The average grain size in our samples is of 5-6

Optical Materials EXPRESS

μm, as determined by the linear intercept method. The grain size distribution is uniform over the sample cross-section.

3. Optical spectroscopy

3.1 Optical absorption

The absorption spectrum of the Tm:$(Lu,Sc)_2O_3$ ceramic was measured using a Varian CARY 5000 spectrophotometer (Agilent) with a resolution of 0.2 nm. In addition to RT studies, we measured the absorption spectra at 6 K using an Oxford Instruments Ltd. cryostat (Model SU 12) with He-gas close-cycle flow. From the absorption coefficient α_{abs} measured at RT, we calculated the RT absorption cross-section, $\sigma_{abs} = \alpha_{abs}/N_{Tm}$, where $N_{Tm} = 13.8 \times 10^{20}$ cm^{-3} corresponds to 4.76 at.% Tm doping.

The transmission of the laser-grade polished 3 mm-thick Tm:$(Lu,Sc)_2O_3$ ceramic sample measured at 2.15 μm (out of the absorption band of Tm^{3+}) was ~77% which is slightly lower than the value arising purely from the Fresnel losses expected for this material (81.1%, if assuming a refractive index n of 1.92). No noticeable distortion or scattering of the probe He-Ne laser beam passing through the sample were detected.

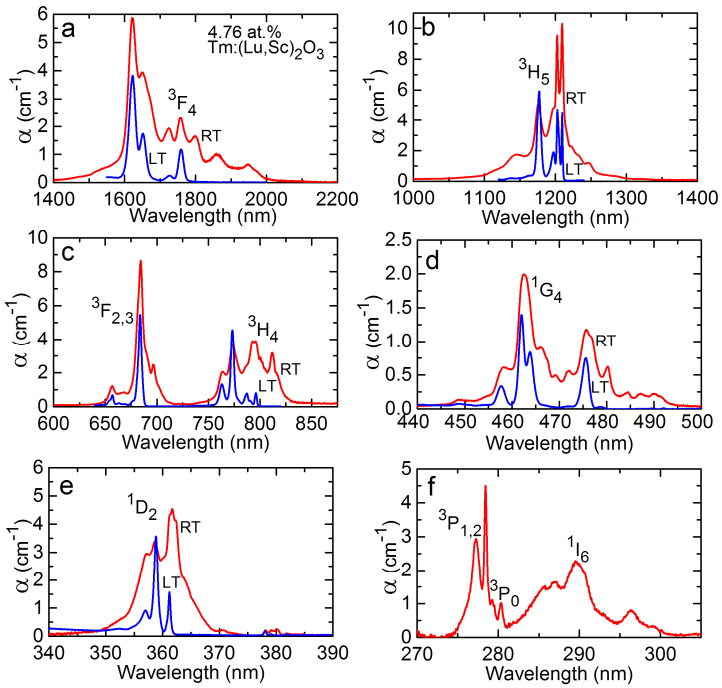

Fig. 3. (a-f) Room-temperature (at 293 K, in *red*) and low-temperature (at 6 K, in *blue*, not in scale) absorption spectra of the 4.76 at.% Tm:$(Lu,Sc)_2O_3$ ceramic.

The RT absorption spectrum is shown in Fig. 3. The absorption band at 1.4-2.1 μm is associated with the $^3H_6 \rightarrow {}^3F_4$ transition of Tm^{3+}. The maximum σ_{abs} for this transition is 4.26 $\times 10^{-21}$ cm^2 at 1622 nm. This band is suitable for in-band pumping of Tm^{3+} ions, e.g., by Raman-shifted Er fiber lasers [25]. The band at 0.74-0.83 μm corresponds to the $^3H_6 \rightarrow {}^3H_4$ transition and it renders the Tm:$(Lu,Sc)_2O_3$ ceramics suitable for pumping with AlGaAs laser diodes. Its maximum σ_{abs} is 2.80 $\times 10^{-21}$ cm^2 at 793 nm with a FWHM of ~25 nm. At shorter wavelengths, the transitions to the $^3F_{2,3}$ (0.64-0.71 μm), $^1G_4$ (0.45-0.49 μm), $^1D_2$ (0.35-0.37 μm) and $^3P_{0\text{-}2} + {}^1I_6$ (0.27-0.30 μm) excited states were also observed. The last one overlaps with the UV absorption edge of the Tm:$(Lu,Sc)_2O_3$ ceramic at $\lambda_g = 282$ nm ($E_g = 4.4$ eV).

Optical Materials EXPRESS

The low-temperature absorption spectra of the Tm:$(Lu,Sc)_2O_3$ ceramic are also shown in Fig. 3 (in blue, not in scale with respect to the RT spectra). Due to the compositional disorder, the absorption spectra are very broad even at 6 K and the transitions to the individual Stark levels are not completely resolved.

The absorption bands of the Tm^{3+} ion in the $(Lu,Sc)_2O_3$ ceramic related to the transitions from the $^3H_6$ ground-state to the excited states from $^3F_4$ to $^1D_2$ were analyzed using the standard Judd-Ofelt (J-O) theory [26,27]. The absorption oscillator strengths were determined from the measured absorption spectra:

$$f_{\Sigma}^{\exp}(JJ') = \frac{m_e c^2}{\pi e^2 N_{\mathrm{Tm}} \langle\lambda\rangle^2} \Gamma(JJ'), \tag{1}$$

where m_e and e are the electron mass and charge, respectively, c is the speed of light, Γ(JJ') is the integrated absorption coefficient within the absorption band and $\langle\lambda\rangle$ is the "center of gravity" of the absorption band. The results are summarized in Table 1.

The values of $f_{\Sigma}^{\exp}$ were used to determine the J-O (intensity) parameters, Ω_k, k = 2, 4, 6: Ω_2 = 2.429, Ω_4 = 1.078 and Ω_6 = 0.653 [10^{-20} cm^2]. Using these parameters, the absorption oscillator strengths were calculated showing a good agreement with the experiment (as indicated by a moderate root-mean-square (rms) deviation, 0.35):

$$f_{\Sigma}^{\mathrm{calc}}(JJ') = \frac{8}{3h(2J'+1)\langle\lambda\rangle} \frac{(n^2+2)^2}{9n} S_{\mathrm{ED}}^{\mathrm{calc}}(JJ') + f_{\mathrm{MD}}^{\mathrm{calc}}(JJ'), \tag{2a}$$

$$S_{\mathrm{ED}}^{\mathrm{calc}}(JJ') = \sum_{k=2,4,6} U^{(k)} \Omega_k, \text{ where } U^{(k)} = \langle (4f^n) SLJ \| U^k \| (4f^n) S'L'J' \rangle^2. \tag{2b}$$

Here, $S_{\mathrm{ED}}^{\mathrm{calc}}$ are the line strengths, h is the Planck constant, n is the refractive index of the crystal and $U^{(k)}$ are the squared reduced matrix elements [28]. The J-O theory describes the electric-dipole (ED) transitions. The contribution of the magnetic-dipole (MD) transition with J–J' = 0, ± 1 (for the $^3H_6 \rightarrow {}^3H_5$ transition), $f_{\mathrm{MD}}^{\mathrm{calc}}$, was taken from [29].

Table 1. Experimental and Calculated Absorption Oscillator Strengths for 4.76 at.% Tm:$(Lu,Sc)_2O_3$ Ceramic

Transition	$\langle\lambda\rangle$, nm	$\langle E\rangle$, cm^{-1}	Γ, cm^{-1}nm	$f_{\Sigma}^{\exp} \times 10^6$	$f_{\Sigma}^{\mathrm{calc}} \times 10^6$
$^3H_6 \rightarrow {}^3F_4$	1709	5851	716.3	2.007	2.053^{ED}
$^3H_6 \rightarrow {}^3H_5$	1190	8401	381.1	2.202	$1.223^{\mathrm{ED}} + 0.525^{\mathrm{MD}}$
$^3H_6 \rightarrow {}^3H_4$	797.52	12539	160.2	2.061	2.150^{ED}
$^3H_6 \rightarrow {}^3F_2 + {}^3F_3$	684.70	14605	118.7	2.072	2.465^{ED}
$^3H_6 \rightarrow {}^1G_4$	467.25	21402	19.9	0.746	0.723^{ED}
$^3H_6 \rightarrow {}^1D_2$	360.05	27774	33.4	2.110	1.897^{ED}
rms deviation					*0.35*

$\langle\lambda\rangle$ - "center of gravity" of the absorption band, $\langle E\rangle$ – Energy barycenter of the multiplet, Γ – integrated absorption coefficient, $f_{\Sigma}^{\exp}$ and $f_{\Sigma}^{\mathrm{calc}}$ – experimental and calculated absorption oscillator strengths (ED + MD), respectively.

3.2 Optical emission

The probabilities for spontaneous radiative transitions were calculated from the corresponding line strengths which were determined from the J-O parameters Ω_k and the squared reduced matrix elements $U^{(k)}$, see Eq. (2b) [28]:

$$A_{\Sigma}^{\mathrm{calc}}(JJ') = \frac{64\pi^4 e^2}{3h(2J'+1)\langle\lambda\rangle^3} n \left(\frac{n^2+2}{3}\right)^2 S_{\mathrm{ED}}^{\mathrm{calc}}(JJ') + A_{\mathrm{MD}}^{\mathrm{calc}}(JJ'). \tag{3}$$

The MD contributions $A_{\mathrm{MD}}^{\mathrm{calc}}$ were taken from [29]. Using the values of $A_{\Sigma}^{\mathrm{calc}}$ for the separate emission channels $J \rightarrow J'$, the total probability, A_{tot}, the corresponding radiative lifetime of the

Optical Materials EXPRESS

excited state, τ_{rad}, and the luminescence branching ratios for the emission channels, $B(JJ')$ were determined:

$$\tau_{rad} = \frac{1}{A_{tot}} \text{ and } B(JJ') = \frac{A_{\Sigma}^{calc}(JJ')}{A_{tot}}, \text{ where } A_{tot} = \sum_{J'} A_{\Sigma}^{calc}(JJ'). \quad (4)$$

The results are shown in Table 2. The calculated radiative lifetime of the lowest excited state is $\tau_{rad}(^3F_4)$ = 4.01 ms. Previously, luminescence decay studies of a 1 at.% Tm:$LuScO_3$ single crystal [30] and a 2 at.% Tm:$LuScO_3$ ceramic [22] revealed a lifetime $\tau_{lum}(^3F_4)$ of 3.84 and 3.2 ms, respectively. The J-O modelling also predicts the radiative lifetime of the $^3H_4$ pump level, $\tau_{rad}(^3H_4)$ = 0.72 ms. In [30] for a 1 at.% Tm:$LuScO_3$ crystal, $\tau_{lum}(^3H_4)$ was measured to be 55 μs while no values for the $LuScO_3$ crystals with lower doping are available (e.g., for 0.2 at.% Tm:Lu_2O_3 crystal, $\tau_{lum}(^3H_4)$ = 300 μs).

The stimulated emission (SE) cross-sections, σ_{SE}, for the $^3F_4 \rightarrow {}^3H_6$ transition of Tm^{3+} in $(Lu,Sc)_2O_3$ ceramic were calculated from the measured absorption spectrum, see Fig. 3(a), using the modified reciprocity method [31]:

$$\sigma_{SE}(\lambda) = \frac{1}{8\pi n^2 \tau_{rad} c} \frac{\sigma_{abs}(\lambda) e^{-hc/(kT\lambda)}}{\int \lambda^{-4} \sigma_{abs}(\lambda) e^{-hc/(kT\lambda)} d\lambda}. \quad (5)$$

Here, k is the Boltzmann constant, T is the crystal temperature (RT), τ_{rad} is the radiative lifetime of the emitting state ($^3F_4$). To reduce the error in σ_{SE} at long wavelengths (> 2 μm) originating from the exponential term in Eq. (5), we additionally used the Füchtbauer–Ladenburg (F-L) equation [32] which is adequate because of the negligible reabsorption in this spectral range, Fig. 3(a). The σ_{SE} spectrum is shown in Fig. 4(a). The maximum σ_{SE} amounts to 7.15×10^{-21} cm^2 at 1951 nm. Above 2 μm where laser operation is expected for low-loss cavities, a local maximum of $\sigma_{SE} = 2.38 \times 10^{-21}$ cm^2 is found at 2090 nm.

Table 2. Calculated Emission Probabilities for Tm^{3+} in $(Lu,Sc)_2O_3$ Ceramic

Excited state	Terminal state	⟨λ⟩, nm	$A_{\Sigma}^{calc}(JJ')$, s^{-1}	$B(JJ')$, %	A_{tot}, s^{-1}	τ_{rad}, ms
$^3F_4$	$^3H_6$	1709	249.15^{ED}	100	249.15	4.01
$^3H_5$	$^3F_4$	3921	$7.25^{ED} + 1.39^{MD}$	2.4	363.35	2.75
	$^3H_6$	1190	$252.51^{ED} + 102.19^{MD}$	97.6		
$^3H_4$	$^3H_5$	2417	$21.74^{ED} + 12.78^{MD}$	2.5	1383.5	0.72
	$^3F_4$	1495	$98.19^{ED} + 28.49^{MD}$	9.2		
	$^3H_6$	797.5	1222.3^{ED}	88.3		
$^3F_2 + {}^3F_3$	$^3H_4$	4840	$5.66^{ED} + 0.31^{MD}$	0.2	2549.2	0.39
	$^3H_5$	1612	344.62^{ED}	13.5		
	$^3F_4$	1142	$67.08^{ED} + 73.34^{MD}$	5.5		
	$^3H_6$	684.7	2058.2^{ED}	80.8		
$^1G_4$	$^3F_2$	1619	15.72^{ED}	0.6	2647.8	0.38
	$^3F_3$	1471	$52.08^{ED} + 4.22^{MD}$	2.1		
	$^3H_4$	1128	$244.76^{ED} + 41.22^{MD}$	10.8		
	$^3H_5$	769.2	$671.99^{ED} + 188.91^{MD}$	32.5		
	$^3F_4$	643.0	$168.92^{ED} + 11.48^{MD}$	6.8		
	$^3H_6$	467.3	1248.5^{ED}	47.2		

⟨λ⟩ - calculated mean wavelength of the emission band, A_{Σ}^{calc} – probability of the radiative spontaneous transition (ED + MD), $B(JJ')$ – luminescence branching ratio, A_{tot} and τ_{rad} – total probability of radiative spontaneous transitions and radiative lifetime of the excited state, respectively

The gain cross-section, $\sigma_g = \beta\sigma_{SE} - (1 - \beta)\sigma_{abs}$, where $\beta = N(^3F_4)/N_{Tm}$ is the inversion ratio, is typically calculated to estimate the expected laser wavelength, see Fig. 4(b). For low β < 0.06, broad and smooth gain spectra are observed centered at ~2.10 μm. For higher β, a peak at 1.97 μm and further one at 1.95 μm dominate the spectrum.

Optical Materials EXPRESS

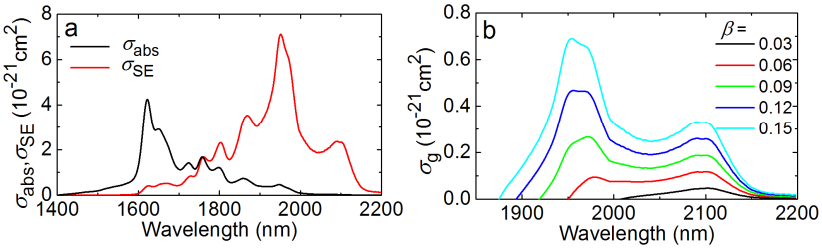

Fig. 4. Spectroscopy of Tm^{3+}-doped $(Lu,Sc)_2O_3$ ceramic: (a) absorption, σ_{abs}, and stimulated-emission, σ_{SE}, cross-sections for the $^3H_6 \leftrightarrow {}^3F_4$ transition; (b) gain cross-sections, $\sigma_g = \beta\sigma_{SE} - (1 - \beta)\sigma_{abs}$, for the $^3F_4 \rightarrow {}^3H_6$ transition. $\beta = N(^3F_4)/N_{Tm}$ is the inversion ratio.

4. Continuous-wave laser operation

4.1 Laser set-up

The laser experiments were performed in a compact microchip-type cavity, Fig. 5(a). The 2.91 mm-thick polished and uncoated Tm:$(Lu,Sc)_2O_3$ ceramic active element (AE) with an aperture of 3.01 × 3.06 mm^2 was mounted in a water cooled (12 °C) Cu-holder. Indium foil was used to provide a better thermal contact from all 4 lateral sides of the AE. The plano-plano cavity consisted of a flat pump mirror (PM) antireflection (AR) coated for 0.77-1.05 μm and high reflection (HR) coated for 1.80-2.12 μm, and a flat output coupler (OC) with transmission of T_{OC} = 1.5%, 3% or 5% at 1.84-2.12 μm. Both PM and OC were placed close to the AE with minimum air gaps, so that the geometrical cavity length was ~3 mm. The AE was pumped through the PM by a fiber-coupled AlGaAs laser diode (LuOcean model Lu0808D200, Lumics, fiber core diameter: 200 μm, NA: 0.22) emitting randomly polarized output at 802 nm (the wavelength was stabilized by water-cooling of the diode). We used a lens assembly (focal length: 30 mm, 1:1 imaging ratio) to focus the pump light into the AE. The radius of the pump beam in the crystal was 100 μm (confocal parameter of the pump beam $2z_R$ = 1.9 mm). The OCs provided a partial reflection (R ≈40%) at the pump wavelength. The total pump absorption under lasing conditions was 48%.

The laser emission spectra were measured with a compact spectrometer (WaveScan, sensitivity: 1.0-2.6 μm, APE GmbH). The beam profile was captured in the far-field using a FIND-R-SCOPE near-IR camera (model 85726, sensitivity: 0.4-2.2 μm), see Fig. 5(b).

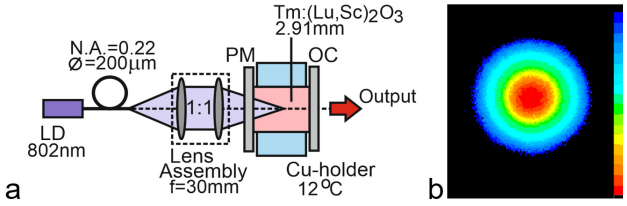

Fig. 5. Tm:$(Lu,Sc)_2O_3$ ceramic microchip laser: (a) scheme of the laser, LD – laser diode, PM – pump mirror, OC – output coupler; (b) laser beam profile captured at P_{abs} = 5.05 W, corresponding to an output power of 1.01 W for T_{OC} = 3%.

4.2 Microchip laser operation

Microchip laser operation has been achieved with all OCs. This indicates a positive thermal lens (and positive dn/dT coefficient) for Tm:$(Lu,Sc)_2O_3$ ceramics. The laser output was randomly polarized. The input-output dependences are shown in Fig. 6(a). The maximum output power reached 1.01 W at 2095-2102 nm with a slope efficiency η = 24% (with respect to the absorbed pump power, P_{abs}) for T_{OC} = 3%. The laser threshold was at P_{abs} = 0.86 W and the optical-to-optical efficiency η_{opt} was 10% (with respect to the incident power). For T_{OC} = 1.5%, slightly lower η = 19% was observed. For both OCs, the output dependence was linear

Optical Materials EXPRESS

up to P_{abs} ~5 W where thermal fracture was observed. For T_{OC} = 5%, the laser output deteriorated (96 mW with η = 8%) which is attributed to stronger upconversion losses and the associated heating. Typical laser emission spectra are presented in Fig. 6(b). The laser emission occurred at ~2.09 μm in agreement with the gain spectra of Tm^{3+} for low inversion ratios β < 0.06, Fig. 4(b). A small β is expected for the utilized low output coupling. The multi-peak spectral behavior is due to etalon effects.

The Tm:$(Lu,Sc)_2O_3$ ceramic microchip laser generated a nearly-circular output beam with a measured $M^2_{x,y}$ < 1.2 (at P_{abs} = 5.05 W, for T_{OC} = 3%), see Fig. 5(b).

As compared with a previous report on a 2 at.% Tm:$LuScO_3$ ceramic emitting at 1982 nm [22], the laser characteristics in the present work are considerably improved. In [22], under diode-pumping at 790 nm, the maximum output power was limited to 211 mW (at P_{abs} ~3.5 W) by thermal roll-over with a slope efficiency of only 8%. Here, despite the higher Tm doping, the ceramic quality allowed to work at higher pump levels to achieve an output power as high as ~1 W at 3 times higher slope efficiency.

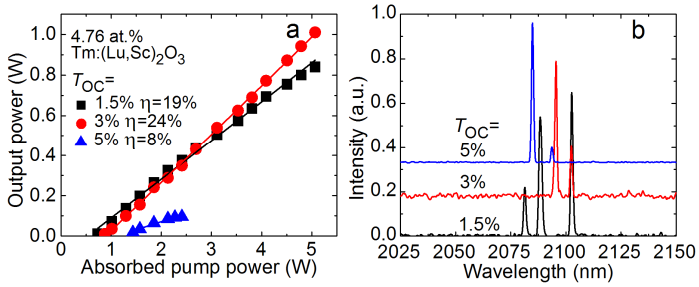

Fig. 6. Tm:$(Lu,Sc)_2O_3$ ceramic microchip laser: (a) input-output dependences, η – slope efficiency; (b) typical laser emission spectra measured at P_{abs} = 5.05 W (for T_{OC} = 1.5% and 3%) and 2.40 W (T_{OC} = 5%).

5. Comparison of ceramics with a single crystal

For the comparative spectroscopic and laser studies, we used a 1.0 at.% Tm:$LuScO_3$ crystal grown by the heat-exchanger method (HEM) [30].

At first, we compare the spectroscopic properties of the single crystal and the ceramic. The absorption cross-section spectra for the $^3H_6 \rightarrow {}^3H_4$ transition are shown in Fig. 7(a). The spectra are similar in shape while less structured for the ceramics. The maximum σ_{abs} of 2.60 × 10^{-21} cm^2 for the Tm:$LuScO_3$ single crystal is observed at 793 nm. It is known that for the Tm^{3+} ion in a "mixed" $LuScO_3$ crystal, σ_{abs} is lower compared to Tm:Lu_2O_3 and Tm:Sc_2O_3 [30] due to a compositional disorder. A similar effect is expected for "mixed" ceramics.

The SE cross-section spectra for the $^3F_4 \rightarrow {}^3H_6$ transition for the single crystal and the ceramic are compared in Fig. 7(b). A slight reduction of σ_{SE} for the ceramic is observed: for the Tm:$LuScO_3$ single crystal, the maximum σ_{SE} is 8.0 × 10^{-21} cm^2 at 1956 nm. The σ_{SE} value for the single crystal determined with the F-L method can be overestimated as compared to that obtained by the reciprocity method in analogy to Tm:Lu_2O_3 [30]. The physical reason is the shorter measured luminescence decay time τ_{lum} for Tm:A_2O_3 crystals than the radiative one τ_{rad}. The peak in the SE cross-section spectra at >2 μm is shifted to a longer wavelength for the Tm:$LuScO_3$ single-crystal (2098 nm) due to the larger fraction of Sc^{3+} ions as compared to the ceramic.

Optical Materials EXPRESS

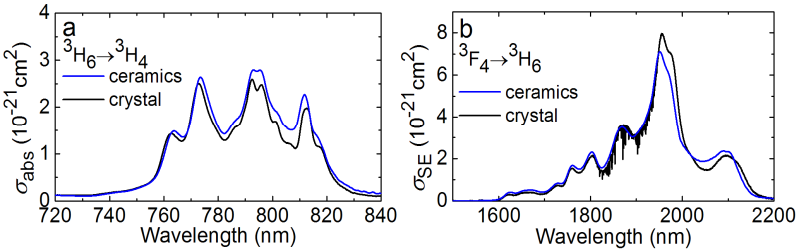

Fig. 7. Spectroscopy of Tm^{3+} in a 4.76 at.% Tm:$(Lu_{2/3}Sc_{1/3})_2O_3$ ceramic and in a 1 at.% Tm:$LuScO_3$ single-crystal: (a) σ_{abs} spectra for the $^3H_6 \rightarrow {}^3H_4$ transition, (b) σ_{SE} spectra for the $^3F_4 \rightarrow {}^3H_6$ transition. The noise of the black curve in (b) is due to water absorption affecting the measured luminescence spectrum.

For the laser experiments with the Tm:$LuScO_3$ single-crystal, we cut a 2.91 mm-thick cubic active element with an aperture of 2.82 × 3.13 mm^2. It was polished to laser-grade quality and remained uncoated. The experiments were performed in the set-up depicted in Fig. 5(a). Microchip laser operation has been achieved and the results are presented in Fig. 8. Due to the observed degradation of the Tm:$LuScO_3$ laser output for T_{OC} > 3%, we additionally studied a high-reflective OC (T_{OC} = 0.2%). The laser emission was randomly polarized. The output power reached 221 mW at 2092-2095 nm with η = 21% for T_{OC} = 1.5%. The laser threshold was at P_{abs} = 0.38 W and η_{opt} was 7%.

Previously, a similar crystal with a thickness of 3 mm was studied under Ti:Sapphire pumping at 796 nm [15,30]. The output power was 324 mW at 1978-1992 nm with η = 40% (for T_{OC} = 1.5%). This is comparable to our result considering the better quality of the pump beam from the Ti:Sapphire laser. Using a 7.7 mm-thick sample, the same authors extracted 705 mW at 2090-2115 nm with η = 55% (at a maximum P_{abs} = 1.4 W) [30].

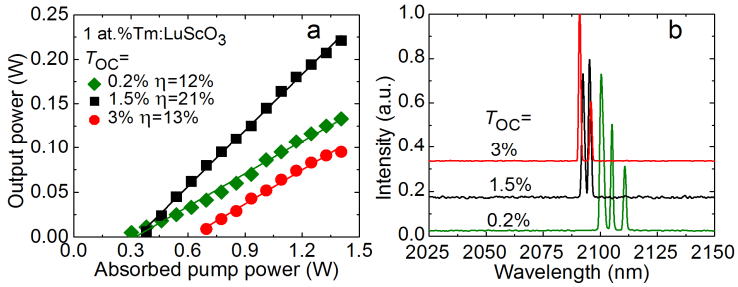

Fig. 8. Tm:$LuScO_3$ single crystal microchip laser: (a) input-output dependences, η – slope efficiency; (b) typical laser emission spectra measured at P_{abs} = 1.41 W.

6. Conclusion

"Mixed" sesquioxide Tm:$(Lu,Sc)_2O_3$ transparent ceramics produced by the HIP method are promising materials for broadly tunable CW and ultrashort (femtosecond) ML oscillators at 1.95-2.1 μm. They allow for high Tm^{3+} doping levels by keeping the optical quality high, size-scalable synthesis, and similar spectroscopic properties as compared to those for HEM-grown Tm:$LuScO_3$ single crystals. In the present work, we report on the first transparent ceramics with composition $(Lu_{2/3}Sc_{1/3})_2O_3$ doped with 4.76 at.% Tm. Their morphology, structure and vibronic properties are studied. The transition probabilities of Tm^{3+} ions are determined within the J-O theory. The ceramic provides broad and smooth gain spectra at 1.9-2.15 μm, as well as relatively high stimulated-emission cross-section at >2 μm, namely 2.38 × 10^{-21} cm^2 at 2090 nm. Using the Tm:$(Lu,Sc)_2O_3$ ceramic in a compact diode-end-pumped microchip laser, watt-level output at ~2.1 μm has been achieved with a slope efficiency of 24%, representing the highest output power demonstrated for any Tm^{3+}-doped $(Lu,Sc)_2O_3$ crystalline or ceramic laser material.

Optical Materials EXPRESS

Funding

Spanish Government (MAT2016-75716-C2-1-R, (AEI/FEDER,UE); MAT2013-47395-C4-4-R, TEC 2014-55948-R); Generalitat de Catalunya (2014SGR1358).

Acknowledgments

W. J. acknowledges financial support from the Key Laboratory of Science and Technology on High Energy Laser, CAEP. F.D. acknowledges additional support through the ICREA academia award 2010ICREA-02 for excellence in research. P. L. acknowledges financial support from the Government of the Russian Federation (Grant No. 074-U01) through ITMO Post-Doctoral Fellowship scheme. P. L. expresses his gratitude to Dr. Christian Kränkel (Institut für Laser-Physik, Universität Hamburg) for providing a Tm:$LuScO_3$ single-crystal and the information about its spectroscopic properties, as well as for the fruitful discussion.